Earthquakes and Structures, *Vol. 27, No. 6 (2024) 517-528*
https://doi.org/10.12989/eas.2024.27.6.517

Research on dynamic response of orthogonal tunnel lining under earthquake

Chen Yang[1], Zelin Lu*[2] and Yinwen Wang[2]

[1]School of Civil Engineering, Sichuan University Jinjiang College, Meishan 620860, China
[2]School of Civil Engineering, Qingdao University of Technology, Qingdao 266520, China

(Received November 4, 2023, Revised November 22, 2023, Accepted October 20, 2024)

Abstract. Relying on the metro line 4 interval tunnel in Chongqing, the dynamic response of orthogonal tunnels at different locations under the influence of horizontal seismic wave sat different time intervals are studied with an earthquake of intensity VIII. By analysis the ANSYS numerical model simulation results and actual monitoring results, the following conclusions can be derive. (1) The lining stress change shows a positive parabolic phenomenon, and the optimal spacing of the upper and lower tunnels can be derived from the stress change as 1.5 times the hole diameter. (2) By studying the displacement values of the monitoring points in the orthogonal tunnel with different spacing between the upper and lower tunnels, it can be seen that the displacement in the horizontal direction of each monitoring point is significantly larger than that in the vertical direction, which leads to the conclusion that the seismic wave in the horizontal direction has a greater effect on the horizontal direction of the tunnel lining. (3) The upper tunnel is most affected by seismic waves at the arch top, followed by the arch waist and the arch foot, and finally the arch bottom. (4) The peak of horizontal displacement in the orthogonal tunnel under the action of horizontal seismic waves is 20 m from the portal of the upper tunnel, rather than the orthogonal part. The research results can provide a helpful manual for the design and construction of orthogonal tunnels in earthquake areas.

Keywords: dynamic response; numerical simulation; seismic wave; tunnel

1. Introduction

Sichuan is a high earthquake prone in China, and there have been five earthquakes of magnitude 6 or higher since the Wenchuan earthquake in 2008 (Fu *et al.* 2020, Sun *et al.* 2022, Yang *et al.* 2014) which have caused great damage to a large number of underground structures and brought huge safety hazards and significant economic losses to the country and its people (Wu *et al.* 2020, Zhang and Jin, 2008). Especially in recent years, a large number of new urban subway tunnels and mountainous highway tunnels have been built (Editorial Department of China Journal of and Transport 2022), and inevitably many orthogonal tunnels with difficult design and construction will be encountered, so it is especially important to study how to improve the seismic resistance of tunnel structures.

The transverse shear deformation induced by seismic waves in one tunnel can subject the adjacent tunnel to a complex stress state involving longitudinal tension, compression, or bending, potentially leading to misalignment or separation between the two tunnels. This indicates that the deformation and stress conditions of closely spaced intersecting subway tunnels under seismic action are more complex, with potentially more severe consequences in terms of structural damage (Chen *et al.* 2010, Zhang *et al.* 2011, Wang *et al.* 2010).To date The impact of new tunnel excavation on existing tunnel structures has been extensively studied (Li *et al.* 2013, Fang *et al.* 2015). Relatively speaking, there is limited published data on the dynamic response of orthogonal tunnel linings to seismic waves. The first shaking table test with an orthogonal tunnel under a landslide as a typical case was carried out to reveal the regional spatial dynamic response characteristics of the lining structure through model deformation characteristics, acceleration, dynamic earth pressure, and dynamic strain time domain characteristics analysis (Pai and Wu 2021). Panthi and Basnet (2019) highlighted the impact of seismic activity on the minimum principal stress in shotcrete-lined high-pressure tunnels at the Upper Tamakoshi Hydroelectric Project (UTHP) in Nepal, influenced by active tectonic movements in the Himalayan region. Innovatively, the study assessed the effect of local shear faults on the minimum principal stress through a combination of field measurements and three-dimensional numerical analysis. Li *et al.* (2014)established a numerical model of a close-fitting cross tunnel using FLAC3D finite difference software, and studied the seismic response characteristics of the close-fitting cross tunnel under strong earthquake by inputting Beijing hotel seismic waves vibrating in the horizontal direction at the model base, and derived different displacement and peak acceleration characteristics of the upper and lower tunnel under strong earthquake. Sun *et al.* (2020) demonstrated through numerical results that the incident angle of P-waves has a significant impact on the peak displacement index and damage extent of hydraulic arch tunnels. Maleska *et al.* (2021) utilized the Tolpinrud railway tunnel in Norway as a

∗Corresponding author, Ph.D.
E-mail: luzelin@qut.edu.cn

http://www.techno-press.com/journals/eas&subpage=7
ISSN: 2092-7614 (Print), 2092-7622 (Online)

case study to investigate the seismic vulnerability of soil-steel composite tunnels. He innovatively proposed a seismic analysis method specifically designed for soil-steel structures and conducted a comparative analysis of the responses of various models under seismic excitation. Mayoral and Mosqueda (2020) conducted a numerical simulation to study the interaction between tunnel-building structural systems in soft soil and its impact on the seismic response of medium-height buildings. The study revealed the actual effects of the presence of the tunnel on the variation of ground motion in the surrounding soil and the seismic performance of the structures. Based on the example of the subway shield tunnel project, Bi *et al.* (2016) developed a three-dimensional finite element model of soil-structure interaction by applying different ground shaking parameters to derive the dynamic response of the lining of an underpass shield tunnel under different ground shaking effects. Besides, some scholars also proposed that the transverse shear deformation occurring in any one of the overlapping tunnels under seismic waves of different propagation directions will result in a complex stress state of bending or tensile compression in the adjacent tunnel (Ding *et al.* 2023, Jishnu and Ayothiraman 2020). The transverse shear deformation will also inevitably lead to irreversible plastic deformation in the overlapping tunnel under the gradual increase of seismic waves (Wu *et al.* 2021, Yang *et al.* 2021, Zhang *et al.* 2019). Thus, it is necessary to study the dynamic response of the lining of orthogonal tunnels with different spacing under seismic action. In addition, the study of the seismic performance of underground orthogonal tunnel structures can summarize universal laws to help the seismic design and construction of practical projects and provide theoretical guidance for future orthogonal tunneling projects.

In this study, based on ANSYS 3D finite element software the orthogonal tunnel model is established with the reference of Chongqing Metro Line 4 interval tunnel under Line 3. The horizontal seismic wave is input in the horizontal direction of the model and the seismic wave vibration direction is perpendicular to the lower tunnel. By observing the variation of acceleration, stress, and displacement at the orthogonal part of the orthogonal tunnel at different spacing, the dynamic response law of the orthogonal part of the orthogonal tunnel at different spacing is derived. The research results can provide a theoretical reference for the design and construction of orthogonal tunnels in earthquake areas.

2. Dynamic response analysis

2.1 Model building

Relying on the metro line 4 interval tunnel in Chongqing, the height, width, and lining thickness of the tunnel are 7.16 m, 7.38 m, and 0.45 m respectively, and the thickness of the overlying soil layer of the upper tunnel structure is 24 m. The upper and lower horseshoe-shaped tunnels of the double-layer orthogonal metro tunnel have the same dimensions, and the lower tunnel structure is orthogonal to the upper tunnel. In order to meet the requirements of computational accuracy and considering the geological conditions of the actual project, a computational model with a side length of 100 m is chosen to establish a positive cube, and the soil model in the finite domain is used to simulate the stresses in the wireless domain (Yan *et al.* 2019, Zlatanovic *et al.* 2015). Viscoelastic artificial boundaries are applied to the front, back, left, and right sides of the model, then all degrees of freedom on the bottom surface of the model are constrained (Jiang *et al.* 2018). According to the geological report, the upper part of the soil uses a class V envelope, while the lower part uses a class IV envelope, simulated using solid185 elements. The lining elements are modeled with shell63 elements. The meshing is performed using a four-node quadrilateral element type, resulting in a total of 4,732 elements and 4,692 nodes, including 130 lining structure elements and 125 nodes. After the model is established, the seismic wave excitation in the horizontal direction is used. The relevant parameters required for the model are shown in Table 1.

Table 1 Physical and mechanical parameters of tunnel surrounding rock and lining

Surrounding rock parameters	Density (kg/m^3)	Modulus of elasticity (GPa)	Poisson's ratio
Level IV	2350	4.76	0.30
Level V	2050	1.31	0.34
Lining	2600	27.51	0.21

The Mohr-Coulomb model is used for the soil layer, and its soil-related parameters can be found in the literature(Fu and Gu 2019). In order to study the degree of influence of different spacing between the upper and lower tunnels of the orthogonal tunnel on the seismic response of the orthogonal part, four different working conditions with the spacing of 0.5, 1.0, 1.5, and 2.0 times the hole diameter are taken in this study to analyze the seismic dynamic response of the orthogonal tunnel under seismic action. The calculation model and the spatial location of the intersecting tunnel are shown in Fig. 1.

2.2 Seismic wave input

The input of ground shaking in this study is the acceleration input method. Since the earthquake intensity used is VIII degrees, the artificial synthetic wave with a peak acceleration is 0.20 g is selected (Liu *et al.* 2023, Ouyang *et al.* 2021) to nitiate the dynamic response analysis by exciting the model from its base along the X-direction. The acceleration reflects the strongest part of the earthquake. Under the same conditions, the higher the acceleration, the stronger the response of the engineering structures. The Code for seismic design of urban rail transit structures (2014) stipulates the selection of seismic wave duration, and it is necessary to ensure that the selected duration should contain peak acceleration and the duration should not be less than 5-10 times the basic period of the structure, so the adjusted acceleration map is shown in Fig. 2.

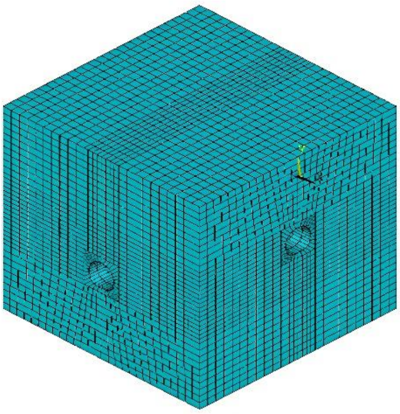

(a) Computational model

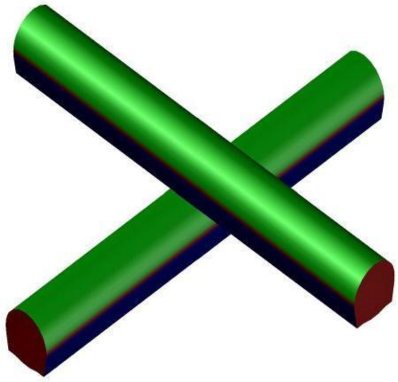

(b) Orthogonal tunnel space location

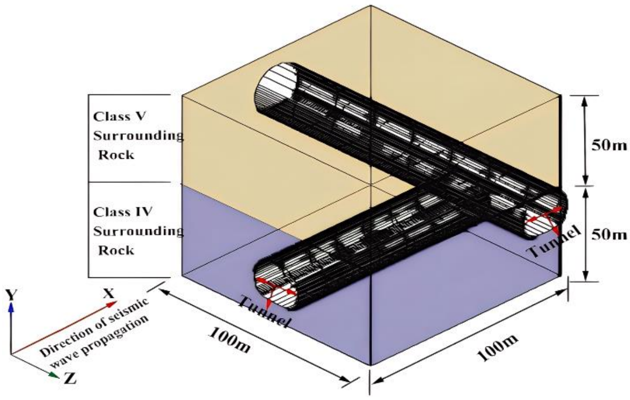

Fig. 1 Calculation model and tunnel space location

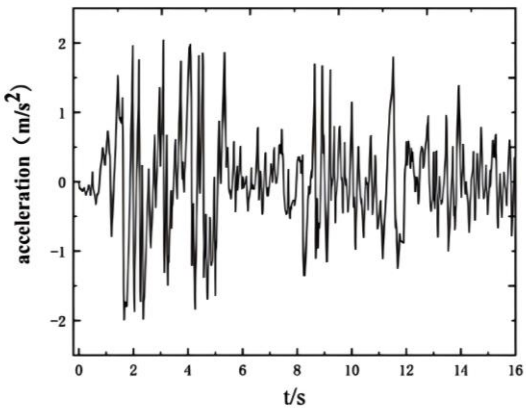

Fig. 2 Input ground vibration acceleration time curve

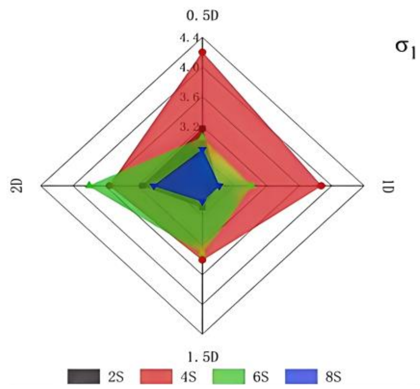

Fig. 4 Peak value of the first principal stress at different moments of the lining

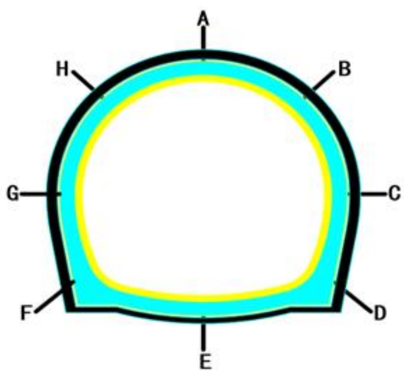

Fig. 3 Orthogonal tunnel stress and displacement monitoring points layout

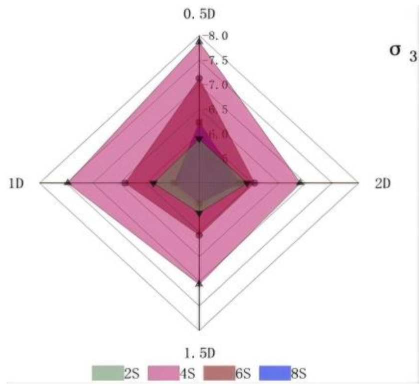

Fig. 5 Peak third principal stress diagram at different moments of lining

Table 2 Peak principal stresses in the lining at different spacing (MPa)

Space \ Time	2 seconds		4 seconds		6 seconds		8 seconds	
	σ1	σ3	σ1	σ3	σ1	σ3	σ1	σ3
0.5 D	3.17	-5.90	4.20	-7.87	3.05	-7.13	2.89	-6.24
1.0 D	2.59	-5.86	3.87	-7.47	3.01	-6.39	2.61	-5.47
1.5 D	2.69	-5.61	3.40	-7.06	3.31	-6.06	2.61	-5.42
2.0 D	3.14	-5.90	3.55	-6.90	3.80	-6.04	3.00	-5.76

Table 3 Peak displacement of each monitoring point at the orthogonal part of the upper and lower tunnels

Spacing between tunnels		Upper side tunnel		Lower side tunnel	
		Horizontal displacement (cm)	Vertical displacement (cm)	Horizontal displacement (cm)	Vertical displacement (cm)
A	0.5D	1.021	-0.264	0.441	-0.002
	1.0D	0.991	-0.004	0.621	0.373
	1.5D	0.911	-0.002	0.539	-0.001
	2.0D	0.862	-0.005	0.484	-0.001
B	0.5D	0.970	-0.193	0.461	-0.012
	1.0D	0.951	0.076	0.591	-0.025
	1.5D	0.871	0.065	0.510	-0.025
	2.0D	0.825	0.063	0.456	-0.024
C	0.5D	0.850	-0.154	0.441	-0.012
	1.0D	0.881	0.082	0.491	-0.017
	1.5D	0.811	0.071	0.422	-0.016
	2.0D	0.782	0.064	0.378	-0.015
D	0.5D	0.720	-0.055	0.361	-0.012
	1.0D	0.811	0.037	0.431	0.072
	1.5D	0.761	0.053	0.357	-0.018
	2.0D	0.748	0.045	0.313	-0.027
E	0.5D	0.650	-0.226	0.341	-0.001
	1.0D	0.811	-0.001	0.431	0.241
	1.5D	0.761	0.002	0.360	0.000
	2.0D	0.749	-0.0004	0.313	-0.0002
F	0.5D	0.740	-0.280	0.331	-0.014
	1.0D	0.841	-0.001	0.451	-0.020
	1.5D	0.811	0.002	0.382	-0.021
	2.0D	0.783	-0.001	0.332	-0.022
G	0.5D	0.880	-0.290	0.311	-0.012
	1.0D	0.931	-0.001	0.571	-0.012
	1.5D	0.871	0.002	0.484	-0.012
	2.0D	0.833	-0.002	0.430	-0.013
H	0.5D	0.990	-0.280	0.391	-0.012
	1.0D	0.991	-0.001	0.631	-0.020
	1.5D	0.911	0.003	0.545	-0.019
	2.0D	0.867	-0.002	0.488	-0.020

3. Analysis of calculation results

To analyze the dynamic response of the orthogonal part of the orthogonal tunnel, this paper monitors the orthogonal key parts (arch top, arch bottom, both sides of the arch waist, and two 45° lines) and some non-orthogonal parts of the orthogonal tunnel, while using different spacing (four working conditions) to compare with each other. The arrangement of each monitoring point in the orthogonal tunnel is shown in Fig. 3.

3.1 Stress analysis

Figs. 4-5 show the peak value of the first main stress and the third main stress of the lining at different moments, in which D represents the tunnel diameter, and the peak stress of the main stress of the lining at different spacing and different moments are shown in Table 2. Principal stress clouds of the orthogonal tunnel lining at different time intervals and spacings are selected for analysis.

The data from the above table gives the peak horizontal stresses of the corresponding monitoring points in the orthogonal tunnel at different spacings and different time intervals. By analyzing the data in the above table, the following conclusions can be derived.

(1) Within the range of 0.5-1.5 times the diameter of orthogonal parts in the orthogonal tunnel, the same main stress of tunnel lining decreases with the increase of spacing. Taking the time interval of 4s as an example, the tensile stress decreases from 4.2 MPa to 3.40 MPa, which is reduced by 19 %. But when the spacing is 1.5-2.0 times the hole diameter, the opposite is true. Taking the time interval of 4s as an example identically, the tensile stress increases from 3.40 MPa to 3.55 MPa, which increases by 1.04 times. It can be seen that the spacing between the upper and lower layers of the orthogonal tunnel is not the larger the better, and 1.5 times the hole diameter spacing is the most reasonable.

(2) As seen from the above table, the stress is higher at points H and B at the vault of the upper tunnel because of the stress concentration, followed by point A. The stress of point G and point C at the arch waist is small, while the stress at the arch foot is the largest due to the influence of the lower tunnel, which can be F>D>E. The lower tunnel is also influenced by the upper tunnel, showing that the stress at the arch top is greater than that at the foot of the arch, and the pattern of stresses at the arch waist is the same as that of the upper tunnel.

3.2 Displacement time course analysis

The data in Table 3 give the horizontal and vertical displacements of the corresponding monitoring points at the orthogonal parts of the upper and lower tunnels under different spacing.

By analyzing the data at each point in Table 3, the following conclusions can be derived.

(1) According to the analysis of the data obtained from the monitoring points of orthogonal parts under different spacing, the displacement in the horizontal direction of each monitoring point is larger than the displacement in the vertical direction, which proves that the effect of seismic waves in the horizontal direction on the displacement of the tunnel lining in the horizontal direction is larger than the effect of displacement in the vertical direction.

(2) The horizontal displacement of monitoring point A in the upper tunnel is much larger than the other points at 0.5 times the hole diameter, reaching 1.021 cm, compared with 0.441 cm in the same monitoring point in the lower tunnel, it can be found that the seismic waves affect the upper tunnel more than the lower tunnel, which is consistent with the results of the close-fitting tunnel study in the literature. The maximum horizontal displacement of the upper tunnel is 2.31 times the maximum horizontal displacement of the lower tunnel, which proves that the upper tunnel is more variable in horizontal displacement compared to the lower tunnel in the orthogonal tunnel.

(3) In the orthogonal tunnel, the horizontal displacement of each monitoring point in the upper tunnel decreases with increasing spacing, but the magnitude of horizontal displacement between different monitoring points at the same spacing shows a positive parabolic variation as shown in Fig. 6. It can be seen from Fig. 6 that the horizontal displacement decreases gradually from A to E, and increases gradually from E to H. The above proves that the arch top of the upper tunnel is most affected by seismic waves, followed by the arch waist and arch foot, and finally the arch bottom.

From the above conclusions, it can be seen that the displacement at point A of the upper tunnel monitoring point is the largest and the stress concentration phenomenon is also more prominent, so the displacement time interval analysis is continued for point A. The horizontal displacement time interval of point A under seismic wave is shown in Fig. 7.

According to the Code for Seismic Design of Urban Rail Transit Structures (2014) in China, it is known that the arch top of the tunnel generates large tensile stresses with the increase of subsidence, which may lead to cracking when the tensile stresses exceed the tolerable tensile stress range of the tunnel lining, so the displacement change of the arch top has been the focus of tunnel research. As shown in Fig. 7, when the spacing between the upper tunnel and the lower tunnel is 0.5 times the diameter of the tunnel, the displacement is the largest, accumulating up to 2.6 cm. However, the monitoring measurement in the new Austrian method stipulates that the cumulative maximum displacement of the arch top cannot exceed 2 cm, so the upper tunnel has a safety hazard. According to the data of the spacing of 0.5 times the hole diameter to 2.0 times the hole diameter, it can be seen that the spacing between the two tunnels of the orthogonal tunnel is too small, which will have a greater adverse effect on the displacement of the arch top of the upper tunnel lining, especially when the spacing is 0.5 times the hole diameter.

In the study of orthogonal tunnels, it is generally recognized that the displacement at the orthogonal site is the largest and most dangerous part, but from the collected displacement data, the deformation of the lining at the upper tunnel entrance under seismic waves should not be neglected. Under the horizontal seismic wave excitation and 0.5 times the hole diameter spacing, the horizontal displacement information of the upper tunnel from 0 m, 5 m, 10 m, 20 m, and 40 m is summarized as follows.

From the analysis of the data in Table 4, the following conclusions can be drawn. The horizontal displacement of each monitoring point of the upper tunnel is in the range of 0-20 m from the entrance, and the value increases with the

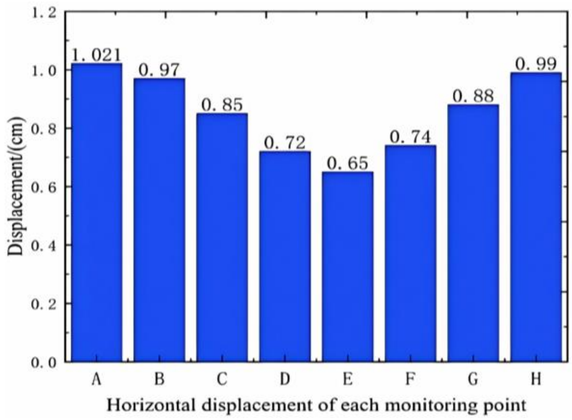

Fig. 6 Variation of horizontal displacement under 0.5 times hole diameter spacing at A-H monitoring point

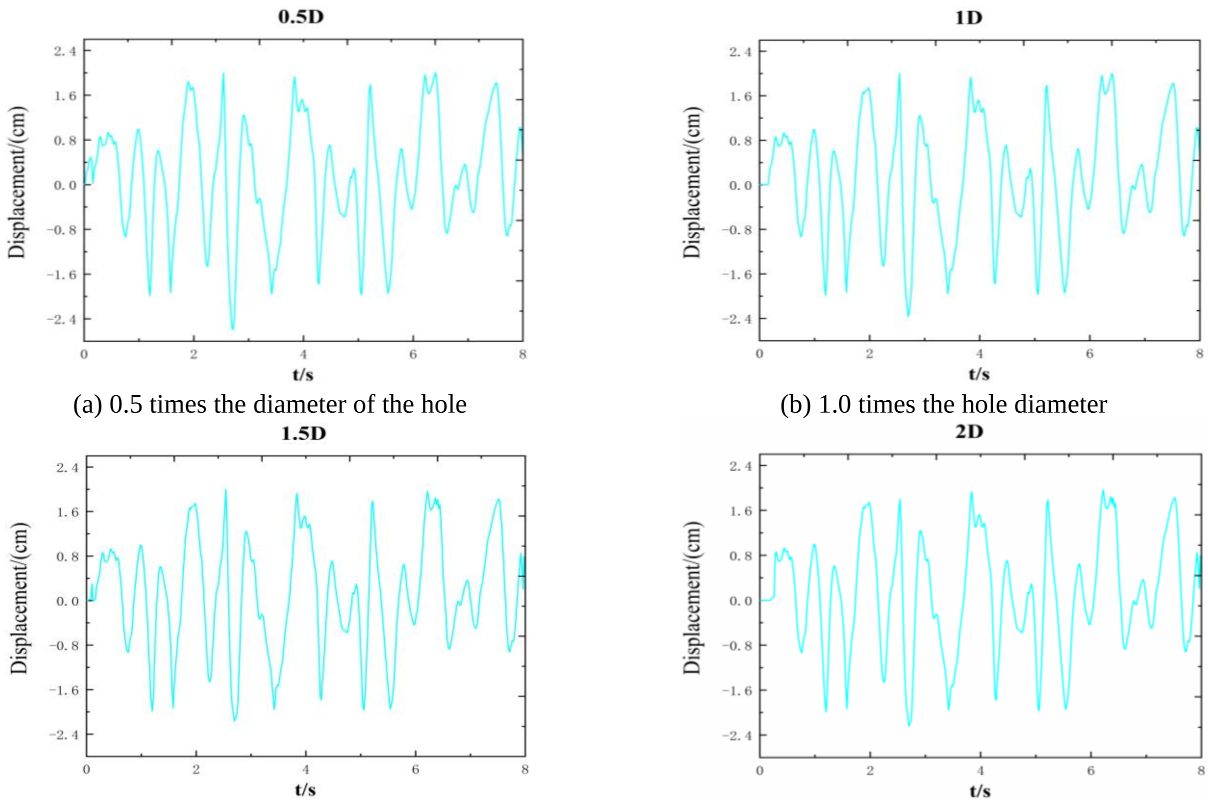

(a) 0.5 times the diameter of the hole (b) 1.0 times the hole diameter

(c) 1.5 times the diameter of the hole (d) 2.0 times the hole diameter

Fig. 7 Upper tunnel lining A point to the horizontal displacement map

Table 4 Horizontal displacement of each monitoring point in the upper tunnel at 0.5 times the hole diameter spacing (cm)

	A	B	C	D	E	F	G	H
0 m	1.021	0.977	0.850	0.716	0.656	0.739	0.823	0.994
5 m	1.078	1.02	0.888	0.748	0.709	0.768	0.919	1.037
10 m	1.097	1.027	0.900	0.767	0.734	0.790	0.935	1.055
15 m	1.111	1.05	0.922	0.802	0.734	0.828	0.970	1.073
20 m	1.110	1.040	0.926	0.813	0.787	0.840	0.968	1.074
40 m	1.015	0.957	0.870	0.792	0.776	0.823	0.918	0.995

increase of distance, and the peak position is about 20 m. Within the range of 20-40 m from the opening, the displacement gradually decreases. Combined with the above research results, it can be concluded that under a

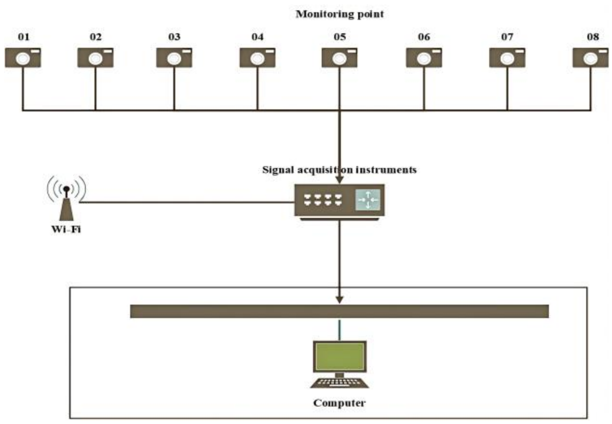

Fig. 8 Displacement data transfer flow chart

Fig. 9 Retrofit monitoring processor

certain distance and horizontal seismic wave excitation the position of the maximum displacement is not in the orthogonal position, but in the range of about 20 m at the entrance of the upper tunnel.

4. Comparative analysis

The interval tunnel of Chongqing Metro Line 4 which is orthogonal to Metro Line 3 has experienced two earthquakes so far, namely the Yaan 7.0 earthquake in 2017 and the Lushan 6.1 earthquake in 2022. To monitor the impact of Line 4 on Line 3 of the existing subway tunnel, a Leica TM30 monitoring robot and several modified monitoring processors were installed at each of the orthogonal parts of Chongqing Metro Line 4 during construction in 2017. Compared with the numerical simulation results, the data collected by these instruments can verify the accuracy of the conclusions. The data transfer process and point layout are shown in Figs. 8-9.

The retrofit monitoring processor is composed of displacement and stress sensors, infrared transmitting and receiving devices, HD cameras, and recorders. The displacement sensor is used to accept small displacement changes in the structure. The stress sensor is to facilitate the collection of internal force changes in the structure lining. The infrared transmitting and receiving device is to form the relative displacement change monitoring by emitting a beam of infrared light to the opposite receiver. The HD cameras are to record the surface changes of the overall tunnel structure. And Leica TM30 monitoring robot is mainly used to automatically monitor the change of displacement monitoring of each monitoring point and the modified monitoring processor's displacement data for comparison.

As shown in Figs. 10-11, when the spacing is 0.5 times the diameter of the hole, the variation in stress at each monitoring point is most pronounced according to the numerical simulation. In the actual project, the minimum spacing between the arch bottom of Line 3 and the arch top of Line 4 is 3.438 m, which is the closest to 0.5 times the diameter of the hole in the numerical simulation. Because the stress change of each monitoring point is the most obvious at this spacing, it is the most appropriate comparison between them.

4.1 Comparative stress analysis

By analyzing the data in Fig. 12, the following conclusions can be derived.

(1) The actual peak data of the first and third principal stresses at each monitoring point in the two earthquakes and the data in the numerical simulation have the same trend. The maximum compressive stresses of the simulated and actual data are 4.32 MPa and 4.3 MPa, both obtained at monitoring point A, while the same is true for the maximum tensile stress. This proves that the site with the greatest stress change under seismic waves in the actual project of the orthogonal tunnel is the arch top, and also indicates that the numerical simulation results are relatively accurate.

(2) The tunnel structure has the most obvious stress concentration at the arch top and the arch bottom under the actual seismic waves, while the stress at the arch waist is smaller. As seen from the chart, the stress change data are consistent with the numerical model results.

4.2 Displacement comparison analysis

The actual monitoring value and numerical simulation value of the displacement peak of each monitoring point of the upper line 3 tunnel when the orthogonal tunnel is subjected to the earthquake are shown in Table 5, and Fig. 13 is the comparison of displacement data.

By analyzing the data for each monitoring point in the above table and figure, the following conclusions can be derived.

(1) Under the action of actual seismic waves, the horizontal displacement of each monitoring point is the same as the numerical simulation data, showing a positive parabolic change. The horizontal displacement value of monitoring point A is the largest, indicating that the seismic wave has a greater impact on the arch top of the upper tunnel than on other parts. The actual data monitored during the construction period are approximately the same as the numerical simulation data, while the actual data monitored during the operation period are significantly smaller than the data monitored during the construction period. From the above analysis, it can be seen that a stable and intact

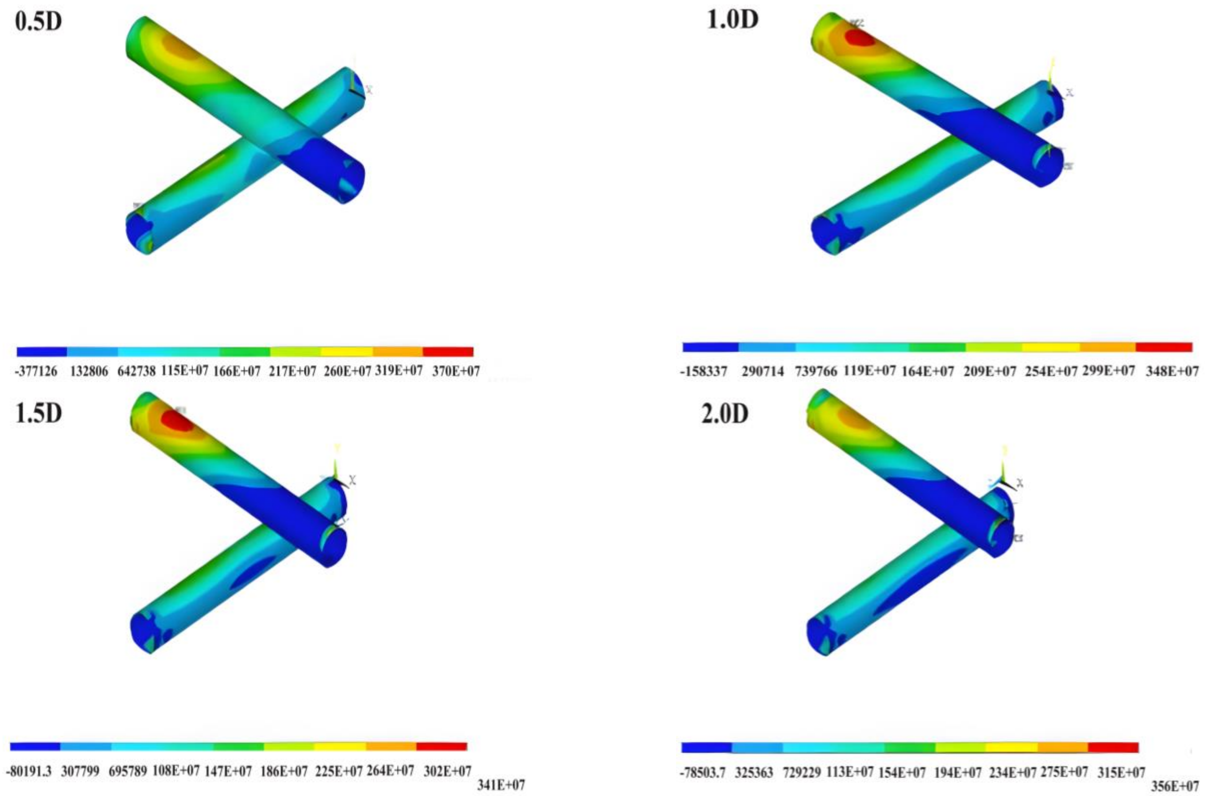

Fig. 10 3D Schematic of the maximum principal stress from numerical simulation

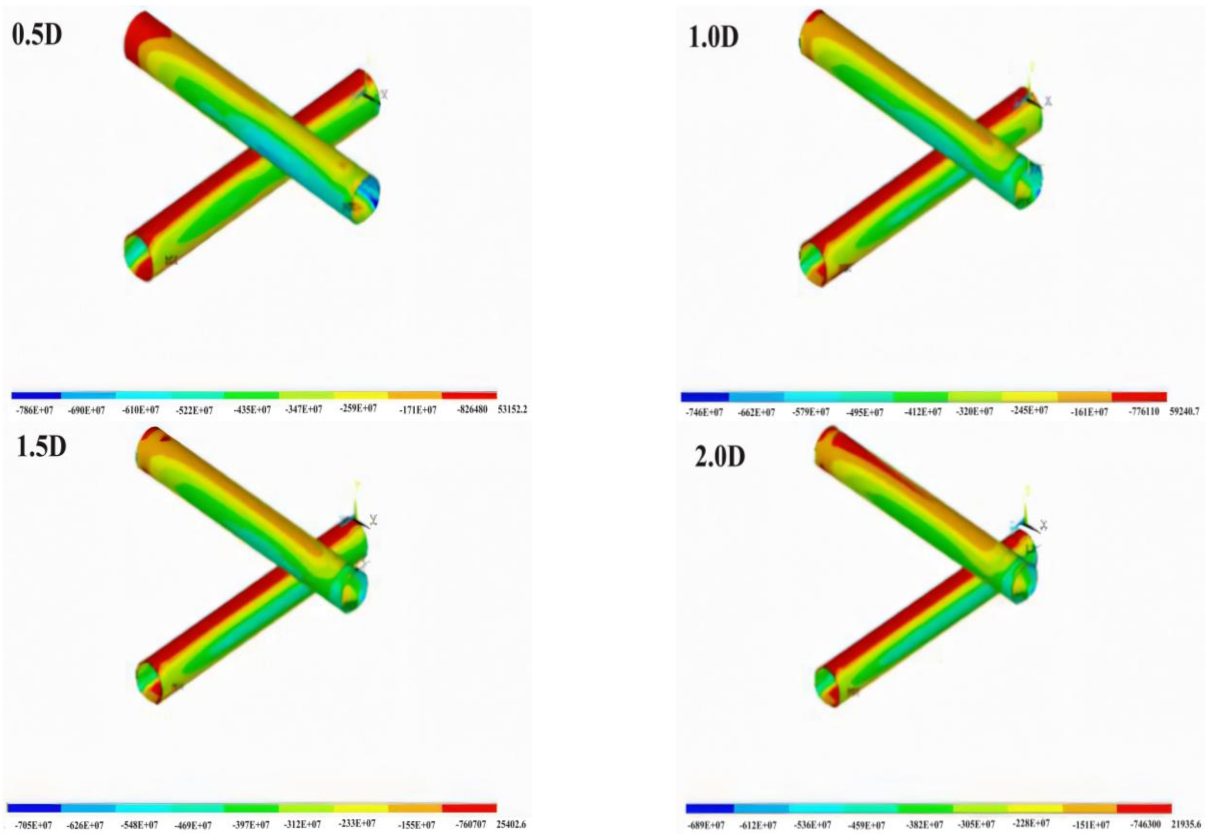

Fig. 11 3D Schematic of the minimum principal stress from numerical simulation

structure helps resist the impact of seismic waves.

(2) Comparing the horizontal displacement with the vertical displacement, it can be concluded that the displacement in the horizontal direction of each monitoring

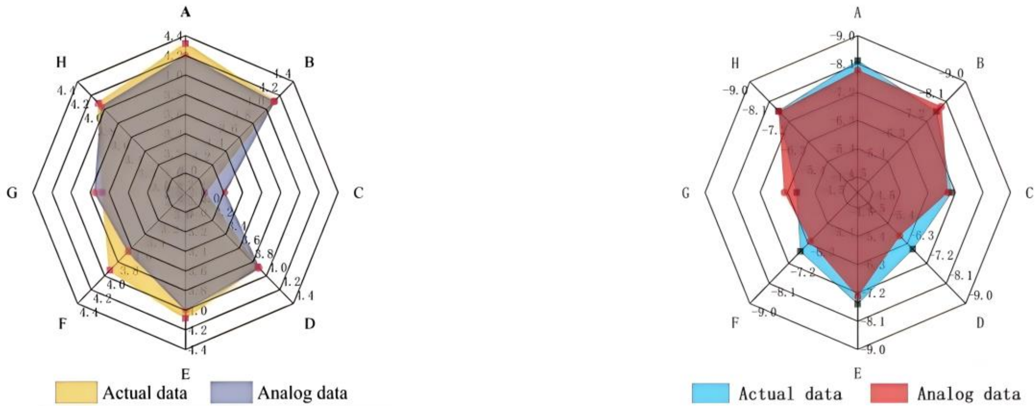

(a) Comparison of the first principal stress peak at the monitoring point
(b) Comparison of the third principal stress peak at the monitoring point

Fig. 12 Comparative graph of stress data (MPa)

Table 5 Comparison of peak displacement data at each monitoring point

Monitoring point	Actual data of construction period (2017)		Actual data of operation period (2022)		Simulation data	
	Horizontal displacement (cm)	Vertical displacement (cm)	Horizontal displacement (cm)	Vertical displacement (cm)	Horizontal displacement (cm)	Vertical displacement (cm)
A	1.121	-0.128	0.42	-0.163	1.021	-0.264
B	1.025	-0.115	0.36	-0.123	0.970	-0.193
C	0.952	-0.085	0.24	-0.114	0.850	-0.154
D	0.812	-0.023	0.28	-0.102	0.720	-0.055
E	0.756	-0.115	0.15	-0.186	0.650	-0.226
F	0.787	-0.108	0.35	-0.106	0.740	-0.280
G	0.985	-0.135	0.30	-0.133	0.880	-0.290
H	1.012	-0.198	0.40	-0.158	0.990	-0.280

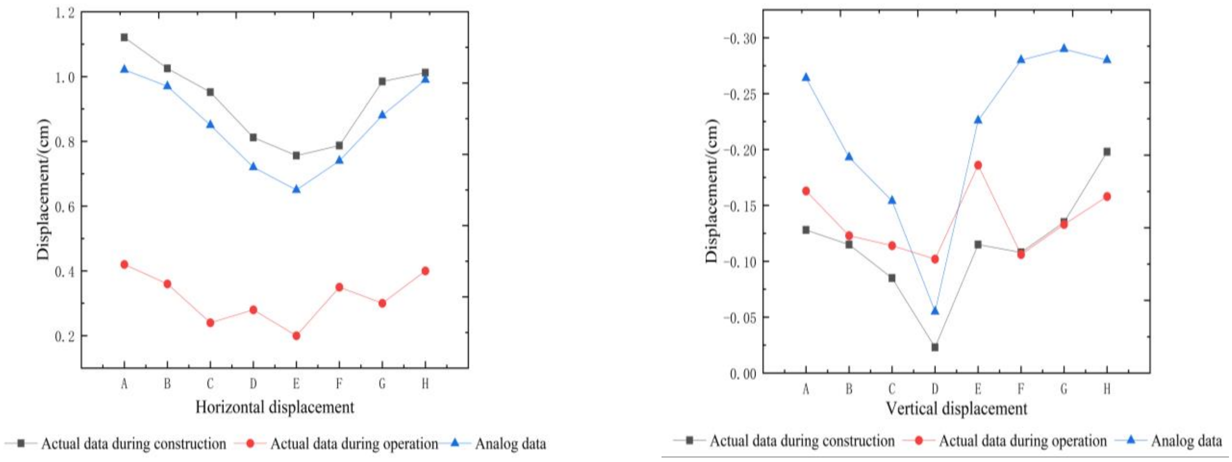

(a) Horizontal displacement comparison chart
(b) Vertical displacement comparison chart

Fig. 13 Comparison chart of displacement data (cm)

point is significantly larger than the displacement in the vertical direction.

(3) The data of each monitoring point in the numerical simulation are closest to the actual measured data during the construction period, which proves that the data obtained from the numerical simulation have some significance.

4.3 Comparative analysis of results from different numerical models

To investigate the differences in dynamic response between various tunnels under seismic loading, this study conducts a comparative analysis of numerical simulation

Table 6 Comparison of dynamic responses of different tunnels under seismic loading

Example	Tunnel Type	Acceleration	Research Method	Stress Results	Displacement Results	Year	Source
Beijing Metro Line 7 Section Tunnel	Double-Layer Crossed Metro Tunnel	0.2 g	Numerical Simulation (FLAC3D)	The maximum stress occurs at the top of the upper tunnel, followed by the middle part	The horizontal displacement at the top of the upper tunnel is greater than that at the corresponding location in the lower tunnel	2014	Li *et al.* (2014)
Hefei Metro Line 2 Section Tunnel	Metro Tunnel	0.15 g	Numerical Simulation	The maximum stress in the tunnel lining structure occurs at the arch crown	The maximum displacement of the tunnel lining structure occurs at the arch crown	2019	Wang *et al.* (2019)
Tawarayama Tunnel	Highway Tunnel	/	Actual Data	The arch crown experiences the highest stress and the most damage	The horizontal displacement at the arch crown is prominent	2018	Zhang *et al.* (2018)
Wenchuan Tunnel Group	Highway Tunnel	0.44 g	Numerical Simulation (ABAQUS)	The maximum stress, and consequently the most severe damage, occurs at the arch shoulders and corners	The maximum displacement occurs at the arch crown	2019	Wang *et al.* (2019)
Chongqing Metro Line 4 Section Tunnel	Orthogonal Metro Tunnel	0.2 g	Numerical Simulation (ANSYS)	The maximum stress occurs at the arch crown of the upper tunnel	The displacement in the horizontal direction is significantly greater than that in the vertical direction	2024	/

results from other research. The comparison results are presented in Table 6.

By comparing the dynamic responses of different tunnels under seismic loading, it is evident that most researchers employ numerical simulation methods to analyze the dynamic responses of tunnels during seismic events. The stress results indicate that the stress at the arch crown is maximized under seismic loading. Furthermore, the comparative analysis of displacement results shows that the horizontal displacement at the arch crown is the greatest

5. Conclusions

5.1 Conclusions

Based on the engineering background of Chongqing Metro Line 4, the dynamic effects of the orthogonal part and the upper tunnel entrance under the influence of horizontal seismic waves are studied. By analyzing the data obtained from the finite element model, the main conclusions are as follows.

(1) Under the action of horizontal seismic waves with different time intervals and different distances between the upper and lower tunnels, the lining stress changes in the orthogonal part of the orthogonal tunnel show a positive parabola phenomenon. When the spacing between the upper and lower tunnels is 0.5-1.5 times the hole diameter, the stress gradually decreases, and when the spacing is 1.5-2.0 times the diameter, the stress gradually increases, which shows that the optimal spacing between the upper and lower tunnels is 1.5 times the hole diameter. From the stress data of local monitoring points, it can be seen that the overall stress in the upper tunnel lining is greater than that in the lower tunnel, with the largest value at the arch top due to stress concentration, followed by the orthogonal part. The maximum stress values at the vault, as determined from numerical simulation and actual monitoring, are 4.32 MPa and 4.3 MPa.

(2) By studying the displacement of each monitoring point under different spacing between the upper and lower tunnels of the orthogonal tunnel, it can be seen that the displacement of each monitoring point in the horizontal direction is obviously larger than that in the vertical direction under the action of seismic waves in the horizontal direction, indicating that the influence of seismic waves in the horizontal direction on the horizontal displacement of tunnel lining is greater than that in the vertical direction. According to the specific value of each monitoring point, it can be seen that the upper tunnel is more affected by horizontal seismic waves than the lower tunnel.

(3) In the orthogonal tunnel, the horizontal displacement of each monitoring point in the upper tunnel decreases with the increase of the spacing, but the magnitude of the horizontal displacement between different monitoring points at the same spacing shows a positive parabolic variation. It is obtained that the arch top of the upper tunnel is most affected by seismic waves, followed by the arch waist and the arch foot, and finally the bottom of the arch.

(4) The horizontal displacement value of each monitoring point in the upper tunnel increases with increasing distance in the range of 0-20 m from the portal, and its peak value mostly appears in the distance of about 20 m from the cave entrance. Within the distance of 20-40 m from the portal, the horizontal displacement of each point decreases with the increase of distance. Combined with the peak displacement of each point in the orthogonal part, it can be seen that the maximum horizontal displacement of the orthogonal tunnel under the action of horizontal seismic waves appears at the upper tunnel 20 m away from the

entrance, rather than the orthogonal part.

5.2 Recommendations

(1) When designing new orthogonal tunnel systems, engineers should prioritize maintaining a spacing between the upper and lower tunnels that is approximately 1.5 times the tunnel diameter. This spacing optimizes stress distribution and reduces stress concentration, thereby enhancing the overall structural stability of the tunnels during seismic events.

(2) During construction, additional reinforcement should be considered for the upper tunnel, particularly at critical locations such as the arch crown. Engineers should utilize higher-strength materials or incorporate additional support structures to withstand these stresses, thereby enhancing the overall seismic resilience of the tunnel system.

(3) For urban tunnels exposed to seismic risk, engineers should implement advanced horizontal displacement mitigation techniques, such as flexible joints or shock-absorbing materials, particularly in areas of the upper tunnel where displacement is more pronounced.

(4) During the construction of orthogonal tunnels, additional reinforcement measures should be implemented within the critical 20-meter zone at the tunnel entrance. These measures could include enhanced supports or specialized seismic damping systems to prevent excessive displacement during seismic events.

Data availability statement

All data included in this study are available upon request by contact with the corresponding author.

Acknowledgments

The APC was funded by Sichuan University Jinjiang College. We thank Professor Gao Feng (Chongqing Jiaotong University) for providing project support, and Dr. Guangzhao Zhang (Qingdao University of Technology) for proofreading the language of this paper.

Conflicts of interest

No potential conflict of interest was reported by the authors.

Reference

Bi, R., Tang, X. and Liu, B. (2016), "Three-dimensional seismic response analysis of a shield-shaped subway tunnel", *Geol. Explor.*, **52**, 712-717. https://doi.org/10.13712/j.cnki.dzykt.2016.04.012.

Chen, L., Chen, G.X. and Long, H. (2010), "3D refined nonlinear finite element analysis of intersecting metro tunnels under near-field ground motion", *Rock Soil Mech.*, **31**, 280-285.

Ding, L.X., Shao, G.B., Shang, J.H. and Han, J.Y. (2023), "Study on transverse seismic response characteristics of large diameter vertical double-layer overlapping pipe jacking in the soil-rock composite stratum", *Appl. Sci. Basel*, **13**, 14. https://doi.org/10.3390/app13042343.

Editorial Department of China Journal of Highway and Transport (2022), "Review on China's traffic tunnel engineering research: 2022", *Chin. J. Highw. Transp.*, **35**(4), 1-40. https://doi.org/10.19721/j.cnki.1001-7372.2022.04.001.

Fang, Q., Zhang, D., Li, Q. and Wong, L.N.Y. (2015), "Effects of twin tunnels construction beneath existing shield-driven twin tunnels", *Tunnell. Undergr. Sp. Technol.*, **45**, 128-137. https://doi.org/10.1016/j.tust.2014.10.001.

Fu, D. and Gu, Y. (2019), "Research on seismic response of mountain tunnel considering soil-structure dynamic interaction", *J. Guangxi Univ. (Nat. Sci. Edit.)*, **44**, 176-182. https://doi.org/10.13624/j.cnki.issn.1001-7445.2019.0176.

Fu, X., Zhu, Q., Liu, C., Li, N.W., Zhuang, W.H., Yang, Z.L., Lu, H. and Tang, M. (2020), "Estimation of landslides and road capacity after August 8, 2017, MS7.0 Jiuzhaigou earthquake using high-resolution remote sensing images", *Adv. Civil Eng.*, **2020**, 11. https://doi.org/10.1155/2020/8828385.

GB 50909-2014 (2014), Code for Seismic Design of Urban Rail Transit Structures, Ministry of Housing and Urban-Rural Development of the People's Republic of China, Beijing, China.

Jiang, X., Wang, F., Yang, H., Sun, G. and Niu, J. (2018), "Dynamic response of shallow-buried small spacing tunnel with asymmetrical pressure: Shaking table testing and numerical simulation", *Geotech. Geol. Eng.*, **36**, 2037-2055. https://doi.org/10.1007/s10706-017-0444-0.

Jishnu, R.B. and Ayothiraman, R. (2020), "Interaction of urban underground twin metro tunnels under static and earthquake loading", *J. Earthq. Tsunami*, **14**, 36. https://doi.org/10.1142/s1793431120500190.

Li, J., Tao, L., Wu, B., An, J. and Guo, F. (2014), "Analysis of 3D dynamic response of closely overlapping tunnels during a strong earthquake", *Modern Tunnell. Technol.*, **51**(1), 26-31.

Li, X.G., Zhang, C.P. and Yuan, D.J. (2013), "An in-tunnel jacking above tunnel protection methodology for excavating a tunnel under a tunnel in service", *Tunnell. Undergr. Sp. Technol.*, **34**, 22-37. https://doi.org/10.1016/j.tust.2012.10.004.

Liu, S.F., Yao, L.Y., Feng, X.J. and Wang, P. (2023), "Response analysis of curved tunnel under near-field long-period ground motion considering seismic wave propagation effect", *Sustainab.*, **15**, 14. https://doi.org/10.3390/su15010060.

Maleska, T., Beben, D. and Nowacka, J. (2021), "Seismic vulnerability of a soil-steel composite tunnel - Norway Tolpinrud railway tunnel case study", *Tunnell. Undergr. Sp. Technol.*, **110**, 18. https://doi.org/10.1016/j.tust.2020.103808.

Mayoral, J.M. and Mosqueda, G. (2020), "Seismic interaction of tunnel-building systems on soft clay", *Soil Dyn. Earthq. Eng.*, **139**, 13. https://doi.org/10.1016/j.soildyn.2020.106419.

Ouyang, Z.Y., Cui, J., Luo, R.F. and Li, P.J. (2021), "Shaking table model test of immersed tunnels with different site conditions and seismic wave input directions", *Ships Offshore Struct.*, **16**, 20-32. https://doi.org/10.1080/17445302.2020.1829372.

Pai, L.F. and Wu, H.G. (2021), "Multi-attribute seismic data spectrum analysis of tunnel orthogonal underpass landslide shaking table test", *Soil Dyn. Earthq. Eng.*, **150**, 17. https://doi.org/10.1016/j.soildyn.2021.106889.

Panthi, K.K. and Basnet, C.B. (2019), "Evaluation of earthquake impact on magnitude of the minimum principal stress along a shotcrete lined pressure tunnel in Nepal", *J. Rock Mech. Geotech. Eng.*, **11**, 920-934. https://doi.org/10.1016/j.jrmge.2019.06.003.

Sun, B.B., Zhang, S.R., Cui, W., Deng, M.J. and Wang, C. (2020), "Nonlinear dynamic response and damage analysis of hydraulic arched tunnels subjected to P waves with arbitrary incoming angles", *Comput. Geotech.*, **118**, 14. https://doi.org/10.1016/j.compgeo.2019.103358.

Sun, B.T., Spencer, B.F., Yan, P.L., Chen, X.Z. and Zhang, G.X. (2022), "Analysis of the seismic vulnerability of buildings in the Lushan M_s 7.0 earthquake in the Sichuan Province of China", *J. Earthq. Eng.*, **26**, 764-792. https://doi.org/10.1080/13632469.2019.1692742.

Wang, W., Tao, L., Zhang, B., Li, W. and Wei, Y. (2010), "A new method for seismic active pressure calculation of the underground structure", *J. Disaster Prevent. Mitigat. Eng.*, **30**, 620-623. https://doi.org/10.13409/j.cnki.jdpme.2010. 06.013.

Wu, H.G., Lei, H. and Lai, T.W. (2021), "Shaking table tests for seismic response of orthogonal overlapped tunnel under horizontal seismic loading", *Adv. Civil Eng.*, **2021**, 19. https://doi.org/10.1155/2021/6633535.

Wu, W.W., Long, F., Liang, M.J., Wei, Y.L., Sun, W., Chen, X.F. and Zhao, J. (2020), "Spatial and temporal variations in earthquake stress drops between the 2008 Wenchuan and 2013 Lushan earthquakes", *Acta Geol. Sin. English Edit.*, **94**, 1635-1650. https://doi.org/10.1111/1755-6724.14582.

Yan, Q.X., Bao, R., Chen, H., Li, B.J., Chen, W.Y., Dai, Y.W. and Zhou, H.Y. (2019), "Dynamic response and waterproof property of tunnel segmental lining subjected to earthquake action", *Earthq. Struct.*, **17**, 411-424. https://doi.org/10.12989/eas.2019.17.4.411.

Yang, J., Chen, J.H., Liu, H.L. and Zheng, J.C. (2014), "Comparison of two large earthquakes in China: The 2008 Sichuan Wenchuan earthquake and the 2013 Sichuan Lushan earthquake", *Nat. Hazards*, **73**, 1127-1136. https://doi.org/10.1007/s11069-014-1121-8.

Yang, T., Rao, Y.K., Wu, H.G., Zhang, J.Y., Lei, H. and Ding, H.J. (2021), "Dynamic response of parallel overlapped tunnel under seismic loading by shaking table tests", *Shock Vib.*, **2021**, 15. https://doi.org/10.1155/2021/2535762.

Zhang, B., Tao, L., Jia, F., Wang, W. and Li, W. (2011), "Analysis of response to horizontal earthquake loading for metro crossing tunnels with super closed distance apart", *Railw. Eng.*, **2011**, 47-50.

Zhang, J.H., Yuan, Y., Bao, Z., Yu, H.T. and Bilotta, E. (2019), "Shaking table tests on the intersection of cross passage and twin tunnels", *Soil Dyn. Earthq. Eng.*, **124**, 136-150. https://doi.org/10.1016/j.soildyn.2019.05.035.

Zhang, M.Z. and Jin, Y.J. (2008), "Building damage in Dujiangyan during Wenchuan earthquake", *Earthq. Eng. Eng. Vib.*, **7**, 263-269. https://doi.org/10.1007/s11803-008-0870-3.

Zlatanovic, E., Lukic, D.C., Prolovic, V., Bonic, Z. and Davidovic, N. (2015), "Comparative study on earthquake-induced soil-tunnel structure interaction effects under good and poor soil conditions", *Eur. J. Environ. Civil Eng.*, **19**, 1000-1014. https://doi.org/10.1080/19648189.2014.992548.

CC